Steady and Unsteady Solutions of Free Convective Micropolar Fluid Flow Near the Lower Stagnation Point of a Solid Sphere

Debasish Dey and Rupjyoti Borah

Abstract An attempt has been done to study the dual solutions (steady and unsteady solutions) of free convective micropolar fluid flow near the stagnation point of a sphere. Governing equations are solved numerically using suitable similarity transformations and MATLAB built-in bvp4c solver technique. The results are discussed graphically for various values of conjugate parameter (corresponds to convective boundary condition) and material parameter for micropolar fluid. Numerical results of wall temperature and skin friction coefficient are represented by tables. During time-dependent case, skin friction coefficient is controlled by material parameter, but the conjugate parameter enhances skin friction coefficient.

Keywords Convective boundary condition · Lower stagnation point · Micropolar fluid · Solid sphere · Steady and unsteady flow

Nomenclature

$\overline{x}$	Displacement variable along the surface of sphere from lower stagnation point
$\overline{y}$	Displacement variable transverse to $\overline{x}$ axis
$\overline{u}$	Velocity component along $\overline{x}$ axis
$\overline{v}$	Velocity component along $\overline{y}$ axis
$\overline{H}$	Angular velocity of the micropolar fluid
a	Radius of the heated sphere
C_p	Specific pressure
$f'(y)$	Dimensionless velocity
g	Gravitational force
Gr	Grashof number
h_f	Coefficient of heat transfer

D. Dey (✉) · R. Borah
Department of Mathematics, Dibrugarh University, Dibrugarh, Assam, India
e-mail: debasish41092@gmail.com

O. Castillo et al. (eds.), *Applied Mathematics and Computational Intelligence*,
Springer Proceedings in Mathematics & Statistics 413,
https://doi.org/10.1007/978-981-19-8194-4_11

$h(y)$	Dimensionless angular velocity
j	Micro inertia density
k	Vortex viscosity
K	Material or micropolar parameter
k_T	Thermal conductivity
n	Constant
Pr	Prandtl number
T	Temperature
T_f	Temperature of the hot fluid
T_∞	Ambient temperature
t	Time

Greek symbols

β	Coefficient of thermal expansion
ρ	Fluid density
γ_1	Conjugate parameter for convective boundary condition
ψ	Stream function
ϕ	Spin gradient
υ	Kinematic viscosity
μ	Dynamic viscosity
$\theta(y)$	Dimensionless temperature
ω	Eigenvalue parameter

Suffix

0	Initial condition
$'$	Prime which represents the differentiation with respect to y

1 Introduction

The stagnation point flow around a sphere has a large amount of practical significance in engineering and industrial processes. Many researchers have used the mechanics of stagnation point flow using different constitutive models due to its wide range of applications in science and engineering. Theory of micropolar fluid flow is applied in microdevices, defectoscopy (diagnostic method for identification of defects), living organisms, etc. Eringen [1] has introduced the theory of micropolar fluid. Ariman et al. [2] and Rees and Bassom [3] have studied fluid flow problems using micropolar

fluid model. Analysis of mixed convective boundary layer flow past a sphere has been done by Chen and Mucoglu [4]. Kadim et al. [5] have investigated the natural convective boundary layer flow past a sphere using a viscoelastic fluid model. Nazar et al. [6, 7] have investigated the micropolar fluid flow past a sphere by taking constant heat flux and wall temperature, respectively. Cheng [8] has investigated the heat and mass transfer effects on micropolar fluid flow past a sphere.

Markin [9] has considered the buoyancy effects on viscous fluid flow with Newtonian heating past vertical plate. Recently, Salleh et al. [10] have investigated the free convection boundary layer flow past a heated sphere using micropolar fluid model. Many researchers (Aziz [11], Makinde and Aziz [12], Ishak et al. [13], Markin and Pop [14], Yao et al. [15], Yacob and Ishak [16]) have carried out the solutions of convective boundary layer flow problems. Recently, Mohamed et al. [17] have studied the behavior of stagnation point flow with convection boundary condition. Stagnation point flow with convective boundary condition using micropolar fluid model has been analyzed by Alkasasbeh[a] et al. [18]. Shu and Wilks [19] have investigated the heat transfer features in the thin-film flow over a hot sphere effecting from a cold vertical plane of liquid falling onto the surface. Aziz et al. [20] have investigated the mixed convection boundary layer flow using viscoelastic micropolar fluid model with the effect of magnetic field.

The main objective of this study is to investigate the steady and unsteady solutions of micropolar fluid flow in the vicinity of the point where velocity is zero of a sphere with convective boundary conditions. The governing partial differential equations are renewed into set of ordinary differential equations using appropriate similarity transformations and have been solved numerically by MATLAB built-in bvp4c solver technique. A comparison of our work has been made with the results of Alkasasbeh[a] et al. [18] to exemplify the truth of the present work.

2 Mathematical Formulation

Here, free convective two-dimensional boundary layer flow has been considered in the region of stagnation point of a heated sphere with the free stream temperature T_∞, which is subjected to a convective boundary condition. Let "a" be the radius of the heated sphere which is shown in Fig. 1.

Under the boundary layer and Boussinesq approximations, the fundamental equations are (following Aziz [11], Eringen [1], Salleh et al. [10], Alkasasbeh[a] et al. [18]):

$$\frac{\partial(\overline{ru})}{\partial\overline{x}} + \frac{\partial(\overline{rv})}{\partial\overline{y}} = 0, \tag{1}$$

$$\rho\left(\overline{u}\frac{\partial\overline{u}}{\partial\overline{x}} + \overline{v}\frac{\partial\overline{u}}{\partial\overline{y}}\right) = (\mu + k)\frac{\partial^2\overline{u}}{\partial\overline{y}^2} + \rho g\beta(T - T_\infty)\sin(\frac{\overline{x}}{a}) + k\frac{\partial\overline{H}}{\partial\overline{y}}, \tag{2}$$

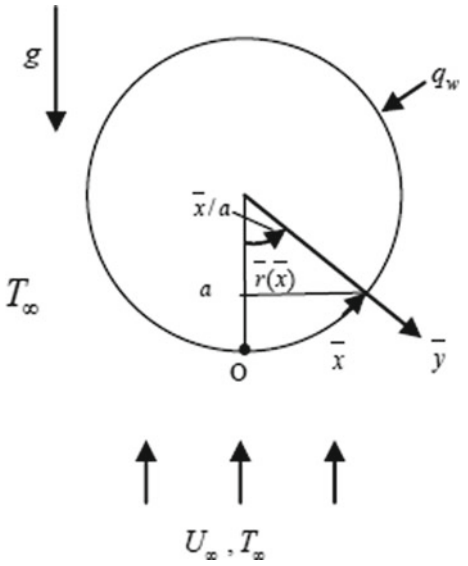

Fig. 1 Flow model

$$\rho j\left(\overline{u}\frac{\partial \overline{H}}{\partial \overline{x}}+\overline{v}\frac{\partial \overline{H}}{\partial \overline{y}}\right)=-k\left(2\overline{H}+\frac{\partial \overline{u}}{\partial \overline{y}}\right)+\phi\frac{\partial^2 \overline{H}}{\partial \overline{y}^2} \tag{3}$$

$$\overline{u}\frac{\partial T}{\partial \overline{x}}+\overline{v}\frac{\partial T}{\partial \overline{y}}=\frac{\upsilon}{\Pr}\frac{\partial^2 T}{\partial \overline{y}^2} \tag{4}$$

and the boundary conditions subject to the above equations are:

$$\left.\begin{array}{l} as\ \ \overline{y}=0:\overline{u}=\overline{v}=0,-k\frac{\partial T}{\partial \overline{y}}=h_f(T_f-T),\overline{H}=-n\frac{\partial \overline{u}}{\partial \overline{y}}, \\ as\ \ \overline{y}\to\infty:\overline{u}\to 0,T\to T_\infty,\overline{H}\to 0, \end{array}\right\} \tag{5}$$

where $\Pr=\frac{\mu C_p}{k_T}$ and h_f the coefficient of heat transfer for the convective boundary conditions and n the constant with $0\le n\le 1$ such that the value $n=0$ which implies $\overline{H}=0$ at the wall physically signifies the concentrated particle flows in which the density of the particle is significantly large that of microelements near the wall are unable to rotate and $n=1$ gives turbulent boundary layer (Ahmadi [21]). In this study, we have considered $n=\frac{1}{2}$ which physically corresponds to vanish the antisymmetric part of the stress tensor and gives the weak concentration of microelements.

Let $\overline{r}(\overline{x})$ be the radial distance which characterizes the distance between the surface of the sphere and symmetrical axis of the sphere which is defined by $\overline{r}(\overline{x})=a\sin(\frac{\overline{x}}{a})$, and ϕ is the spin gradient viscosity that has the following form as proposed by Ahmadi [21]:

$$\phi = (\mu + (\frac{k}{2}))j. \tag{6}$$

Following Salleh et al. [10], Aziz [11], and Alkasasbeh[a] et al. [18], we consider the following dimensionless variables:

$$\left.\begin{array}{l} x = \frac{\bar{x}}{a}, y = Gr^{\frac{1}{4}}(\frac{\bar{y}}{a}), r = \frac{\bar{r}}{a}, u = (\frac{a}{\upsilon})Gr^{-\frac{1}{2}}\bar{u}, v = (\frac{a}{\upsilon})Gr^{-\frac{1}{4}}\bar{v}, \\ H = (\frac{a^2}{\upsilon})Gr^{-\frac{3}{4}}\bar{H}, \theta = \frac{T-T_\infty}{T_f-T_\infty}, \end{array}\right\} \tag{7}$$

where $Gr = \frac{g\beta(T_f-T_\infty)a^3}{\upsilon^2}$ is the Grashof number. Substituting (7) into Eqs. (1–4), we have got

$$\frac{\partial}{\partial x}(ru) + \frac{\partial}{\partial y}(rv) = 0, \tag{8}$$

$$u\frac{\partial u}{\partial x} + v\frac{\partial u}{\partial y} = (1+K)\frac{\partial^2 u}{\partial y^2} + \theta \sin x + K\frac{\partial H}{\partial y}, \tag{9}$$

$$u\frac{\partial H}{\partial x} + v\frac{\partial H}{\partial y} = -K(2H + \frac{\partial u}{\partial y}) + (1+\frac{K}{2})\frac{\partial^2 H}{\partial y^2}, \tag{10}$$

$$u\frac{\partial \theta}{\partial x} + v\frac{\partial \theta}{\partial y} = \frac{1}{\mathrm{Pr}}\frac{\partial^2 \theta}{\partial y^2}, \tag{11}$$

where $K = \frac{k}{\mu}$, and the reduced boundary conditions are

$$\left.\begin{array}{l} \text{as } y = 0 : u = v = 0, \frac{\partial \theta}{\partial y} = -\gamma_1(1-\theta), H = -\frac{1}{2}\frac{\partial u}{\partial y}, \\ \text{as } y \to \infty : u \to 0, \theta \to 0, H \to 0 \end{array}\right\} \tag{12}$$

where $\gamma_1 = \frac{ah_f Gr^{-\frac{1}{4}}}{k}$. It is seen that if $\gamma_1 = 0$, then $\theta = 0$, and therefore, $h_f = 0$ implies that there is no heat supply from the sphere (Salleh et al. [10] and Alkasasbeh[a] et al. [18]).

We introduce the following similarity variables (following Alkasasbeh[a] et al. [18]):

$$\psi = xr(x)f(x,y), \theta = \theta(x,y), H = xh(x,y) \tag{13}$$

where ψ is the stream function, and $u = \frac{1}{r}\frac{\partial \psi}{\partial y}$ and $v = -\frac{1}{r}\frac{\partial \psi}{\partial x}$ satisfy Eq. (8). Further, we have concentrated our main concern to study the flow behavior in the vicinity of lower stagnation point, and mathematical formulations are done using (following Alkasasbeh et al. [18]) $x \approx 0$. Now, substituting Eq. (13) into Eqs. (9–12), the following ordinary differential equations are obtained:

$$(1+K)f''' + 2ff'' - f'2 + \theta + Kh' = 0, \tag{14}$$

$$(1+\frac{K}{2})h'' + 2fh' - f'h - K(2h+f'') = 0, \tag{15}$$

$$\frac{1}{\mathrm{Pr}}\theta'' + 2f\theta' = 0, \tag{16}$$

and the modernized boundary conditions are:

$$\left.\begin{array}{l} f(0) = f'(0), \theta'(0) = -\gamma_1(1-\theta(0)), h(0) = -\frac{1}{2}f''(0), \\ \text{as } y \to \infty : f'(y) \to 0, \theta(y) \to 0, h(y) \to 0. \end{array}\right\} \tag{17}$$

3 Unsteady Flow Case

The unsteady case of this problem is performed to make a comparison between the steady and unsteady flow solutions and help us to characterize which solution of the dual solutions is physically realizable. Weidman et al. [22] and Khashi'ie et al. [23] have investigated that the dual solutions (steady and unsteady cases) exist for the forced convection boundary layer flow past a permeable flat plate and forced convection flow of a non-Newtonian fluid past a wedge, respectively, and suggested that the upper branch (steady solution) solutions are stable in nature and physically realizable and the lower branch (unsteady solution) solutions are not physically acceptable.

To test these features, we consider the unsteady form of Eqs. (1–4), and (1) clearly holds. Equations (2–4) become.

$$\frac{\partial \overline{u}}{\partial \overline{t}} + \rho\left(\overline{u}\frac{\partial \overline{u}}{\partial \overline{x}} + \overline{v}\frac{\partial \overline{u}}{\partial \overline{y}}\right) = (\mu + k)\frac{\partial^2 \overline{u}}{\partial \overline{y}^2} + \rho g\beta(T - T_\infty)\sin(\frac{\overline{x}}{a}) + k\frac{\partial \overline{H}}{\partial \overline{y}}, \tag{18}$$

$$\frac{\partial \overline{H}}{\partial \overline{t}} + \rho j\left(\overline{u}\frac{\partial \overline{H}}{\partial \overline{x}} + \overline{v}\frac{\partial \overline{H}}{\partial \overline{y}}\right) = -k\left(2\overline{H} + \frac{\partial \overline{u}}{\partial \overline{y}}\right) + \phi\frac{\partial^2 \overline{H}}{\partial \overline{y}^2}, \tag{19}$$

$$\frac{\partial T}{\partial \overline{t}} + \overline{u}\frac{\partial T}{\partial \overline{x}} + \overline{v}\frac{\partial T}{\partial \overline{y}} = \frac{\upsilon}{\mathrm{Pr}}\frac{\partial^2 T}{\partial \overline{y}^2}. \tag{20}$$

We consider the following non-dimensionless variables:

$$\left.\begin{array}{l} t = \frac{Gr^{\frac{1}{2}}}{a^2}\overline{t}, x = \frac{\overline{x}}{a}, y = Gr^{\frac{1}{4}}\left(\frac{\overline{y}}{a}\right), r = \frac{\overline{r}}{a}, u = \left(\frac{a}{\upsilon}\right)Gr^{-\frac{1}{2}}\overline{u}, v = \left(\frac{a}{\upsilon}\right)Gr^{-\frac{1}{4}}\overline{v}, \\ H = \left(\frac{a^2}{\upsilon}\right)Gr^{-\frac{3}{4}}\overline{H}, \theta = \frac{T-T_\infty}{T_f-T_\infty}. \end{array}\right\} \tag{21}$$

Using these dimensionless variables in Eqs. (18–20), we get the following partial differential equations:

$$\frac{\partial u}{\partial t}+u\frac{\partial u}{\partial x}+v\frac{\partial u}{\partial y}=(1+K)\frac{\partial^2 u}{\partial y^2}+\theta\sin x+K\frac{\partial H}{\partial y}, \tag{22}$$

$$\frac{\partial H}{\partial t}+u\frac{\partial H}{\partial x}+v\frac{\partial H}{\partial y}=-K(2H+\frac{\partial u}{\partial y})+(1+\frac{K}{2})\frac{\partial^2 H}{\partial y^2}, \tag{23}$$

$$\frac{\partial \theta}{\partial t}+u\frac{\partial \theta}{\partial x}+v\frac{\partial \theta}{\partial y}=\frac{1}{\mathrm{Pr}}\frac{\partial^2 \theta}{\partial y^2}, \tag{24}$$

where t denotes time, and it is important for the question of which solution will be obtained physically realizable. Based on the variables (13), we introduce the new dimensionless variables:

$$\psi=xr(x)f(x,y,t),\theta=\theta(x,y,t),H=xh(x,y,t). \tag{25}$$

Using these variables into Eqs. (18–20), we have got the following nonlinear ordinary differential equations:

$$\begin{aligned}&\frac{\partial^2 f}{\partial y\partial t}+x\frac{\partial f}{\partial y}\frac{\partial^2 f}{\partial x\partial y}+\left(\frac{\partial f}{\partial y}\right)^2-(1+x\cot x)f\frac{\partial^2 f}{\partial y^2}-x\frac{\partial f}{\partial x}\frac{\partial^2 f}{\partial y^2}\\&=(1+K)\frac{\partial^3 f}{\partial y^3}+\frac{\sin x}{x}\theta+K\frac{\partial h}{\partial y},\end{aligned} \tag{26}$$

$$\begin{aligned}&\frac{\partial h}{\partial t}+x\frac{\partial f}{\partial y}\frac{\partial h}{\partial x}+\frac{\partial f}{\partial y}h-(1+x\cot x)f\frac{\partial h}{\partial y}-x\frac{\partial f}{\partial x}\frac{\partial h}{\partial y}\\&=-2Kh-K\frac{\partial^2 f}{\partial y^2}+\left(1+\frac{K}{2}\right)\frac{\partial^2 h}{\partial y^2},\end{aligned} \tag{27}$$

$$\frac{\partial \theta}{\partial t}+x\frac{\partial f}{\partial y}\frac{\partial \theta}{\partial x}-(1+x\cot x)f\frac{\partial \theta}{\partial y}-x\frac{\partial f}{\partial x}\frac{\partial \theta}{\partial y}=\frac{1}{\mathrm{Pr}}\frac{\partial^2 \theta}{\partial y^2}. \tag{28}$$

Again, putting $x\approx 0$, Eqs. (26–28) will reduce to the following equations:

$$\frac{\partial^2 f}{\partial y\partial t}+\left(\frac{\partial f}{\partial y}\right)^2-2f\frac{\partial^2 f}{\partial y^2}=(1+K)\frac{\partial^3 f}{\partial y^3}+\theta+K\frac{\partial h}{\partial y}, \tag{29}$$

$$\frac{\partial h}{\partial t}+\frac{\partial f}{\partial y}h-2f\frac{\partial h}{\partial y}=-2Kh-K\frac{\partial^2 f}{\partial y^2}+\left(1+\frac{K}{2}\right)\frac{\partial^2 h}{\partial y^2}, \tag{30}$$

$$\frac{\partial \theta}{\partial t}-2f\frac{\partial \theta}{\partial y}=\frac{1}{\mathrm{Pr}}\frac{\partial^2 \theta}{\partial y^2}, \tag{31}$$

and the relevant boundary conditions are:

$$\left.\begin{array}{l} f(0,t) = \frac{\partial f}{\partial y}(0,t) = 0,\ \frac{\partial \theta}{\partial y}(0,t) = -\gamma_1(1-\theta(0,t)),\ h(0,t) = -\frac{1}{2}\frac{\partial^2 f}{\partial y^2}(0,t), \\ \text{as } y \to \infty : \frac{\partial f}{\partial y}(y,t) \to 0,\ \theta(y,t) \to 0,\ h(y,t) \to 0. \end{array}\right\} \tag{32}$$

The following representation is taken on to comparison between the dual solutions, according to Weidman et al. [22] and Khashi'ie et al. [23]:

$$\left.\begin{array}{l} f(y,t) = f_0(y) + e^{-\omega t}F(y,t), \\ h(y,t) = h_0(y) + e^{-\omega t}H_1(y,t), \\ \theta(y,t) = \theta_0(y) + e^{-\omega t}G(y,t). \end{array}\right\} \tag{33}$$

where $F(y,t)$, $H_1(y,t)$, and $G(y,t)$ are small relative to the steady flow solutions $f_0(y)$, $h_0(y)$, and $\theta_0(y)$, respectively. The following linearized problems will be obtained by substituting (29) into Eqs. (29–31):

$$\begin{aligned} &(1+K)\frac{\partial^3 F}{\partial y^3} + G(y,t) + K\frac{\partial H_1}{\partial y} + \omega\frac{\partial F}{\partial y} - \frac{\partial^2 F}{\partial y \partial t} \\ &- 2\frac{\partial F}{\partial y} + 2f_0\frac{\partial^2 F}{\partial y^2} + 2F\frac{\partial^2 f_0}{\partial y^2} = 0, \end{aligned} \tag{34}$$

$$\begin{aligned} &\left(1+\frac{K}{2}\right)\frac{\partial^2 H_1}{\partial y^2} - K\left[2H_1 + \frac{\partial^2 F}{\partial y^2}\right] + \omega H_1 - \frac{\partial H_1}{\partial t} + \frac{\partial f_0}{\partial y}H_1 \\ &+ \frac{\partial F}{\partial y}h_0 + 2f_0\frac{\partial H_1}{\partial y} + 2F\frac{\partial h_0}{\partial y} = 0, \end{aligned} \tag{35}$$

$$\frac{1}{\mathrm{Pr}}\frac{\partial^2 G}{\partial y^2} + \omega G - \frac{\partial G}{\partial t} + 2f_0\frac{\partial G}{\partial y} + 2F\frac{\partial \theta_0}{\partial y} = 0 \tag{36}$$

and the boundary conditions are:

$$\left.\begin{array}{l} F(0,t) = \frac{\partial F}{\partial y}(0,t) = 0,\ \frac{\partial G}{\partial y}(0,t) = \gamma_1 G(0,t),\ H_1(0,t) = -\frac{1}{2}\frac{\partial^2 F}{\partial y^2}(0,t), \\ \text{as } y \to \infty : \frac{\partial F}{\partial y}(y,t) \to 0,\ G(y,t) \to 0,\ H_1(y,t) \to 0. \end{array}\right\}. \tag{37}$$

The solutions $f(y) = f_0(y), h(y) = h_0(y)$ and $\theta(y) = \theta_0(y)$ of the steady Eqs. (14–16) are obtained by setting $t = 0$. The function $F(y) = F_0(y)$, $H_1(y) = H_{1_0}(y)$, and $G(y) = G_0(y)$ will identify the initial growth or decay of disturbances of the solutions of Eqs. (34–36). Thus, the linearized eigenvalue problems are given by

$$(1+K)F_0''' + G_0 + KH_{1_0}' + (\omega - 2)F_0' + 2\left(f_0F_0'' + F_0f_0''\right) = 0, \tag{38}$$

$$\left(1+\frac{K}{2}\right)H_{1_0}+\left(f_0'-2+\omega\right)H_{1_0}-KF_0+F_0'+2f_0H_{1_0}+2F_0=0, \tag{39}$$

$$\frac{1}{\mathrm{Pr}}G_0+\omega G_0+2\left(f_0G_0'+F_0\theta_0'\right)=0 \tag{40}$$

Related boundary conditions are:

$$\left.\begin{array}{c} F_0(0)=F_0'(0)=0,\ G_0'(0)=\gamma_1 G_0(0),\ H(0)=-\frac{1}{2}F_0''(0) \\ \text{as } \infty: F(0)\to 0,\ G_0(0)\to 0,\ H_0(0)\to 0 \end{array}\right\} \tag{41}$$

The nature of the steady and unsteady flow solutions depends on the smallest eigenvalue, ω_1. Following Harish et al. [24], we reduce the boundary condition $F_0'(\infty)\to 0$ to a new boundary condition, $F_0(0)=1$, to evaluate the fixed value of eigenvalues and hence solve (38–40).

4 Results and Discussion

The outcome of this work highlights the effect of two parameters, namely the material parameter K and the conjugate parameter γ_1 (parameter responsible for convective boundary condition) on the velocity, angular velocity, and temperature profiles. Here, we have considered $x\approx 0$ (neighborhood of lower stagnation point of the sphere), and the Prandtl number Pr is fixed to 0.7 ($\mathrm{Pr}\ll 1$), which physically indicates the liquid metals-air, which have high thermal conductivity) throughout this paper. We have considered the values of the material parameter $K=0,1,2$, i.e., $K=0$ characterizes Newtonian fluid and nonzero values signify micropolar fluids. Also, we have considered the conjugate parameter $\gamma_1\le 1$, which physically indicates the higher vortex viscosity fluid. All the flow profiles (2–6) have satisfied the convective boundary conditions asymptotically. The visualizations of steady and unsteady flow are emphasized on Figs. 2, 3, 4, 5 and 6. The first solution (steady solution) is denoted by a solid line, and the second solution (unsteady solution) is represented by the dashed line.

Tables 1and 2 represent the numerical results of the first and second solutions of the skin friction coefficient $f(0)$ and wall temperature $\theta(0)$ for $K=0,1,2$ when $\mathrm{Pr}=0.7$ and $\gamma_1=0.05,0.2$. We have compared our first solutions (steady flow) of skin friction coefficient and wall temperature with the work of Alkasasbeh[a] et al. [18] in Tables 1 and 2, respectively.

From these tables, it is seen that for a fixed value of γ_1, skin friction coefficient for time-independent flow experiences reduction in the magnitude with the enhancement of K, but a reverse pattern is experienced during time-dependent fluid flow around a solid sphere. Further, the convective boundary condition helps to magnify skin friction coefficient. The skin friction coefficient of Newtonian fluid flow is more than micropolar fluid flow (steady case), but opposite behavior is observed for unsteady

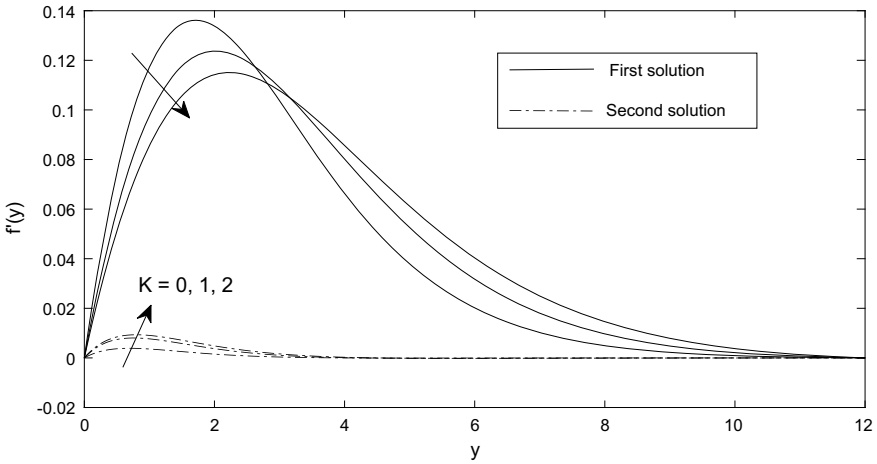

Fig. 2 Velocity distributions $f'(y)$ for some values of K when $\Pr = 0.7$ and $\gamma_1 = 0.05$

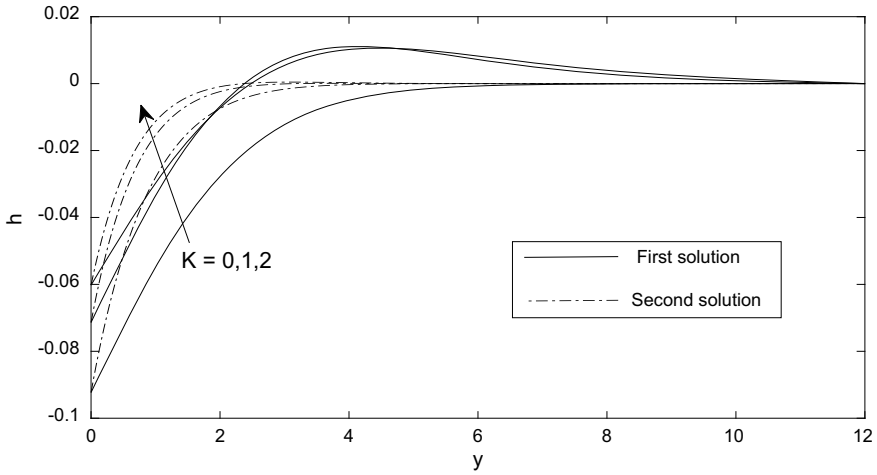

Fig. 3 Angular velocity distributions $h(y)$ for some values of K when $\Pr = 0.7$ and $\gamma_1 = 0.05$

cases. Similarly, temperature of fluid at the surface experiences reduction with K, and it is maximum for Newtonian fluid than micropolar fluids during time-independent cases, but during time-dependent cases, K helps to enhance the wall temperature.

Figures 2 and 3 characterize the influence of material parameter K for $\gamma_1 = 0.05$ and $\Pr = 0.7$ on the velocity and angular velocity in the neighborhood of lower stagnation point of the sphere, $x \approx 0$. Fluid reaches its maximum velocity during $K = 0$ (Newtonian case) and then gradually it decreases because of the presence of vortex viscosity. Small variation between Newtonian and non-Newtonian cases is seen during unsteady fluid flows.

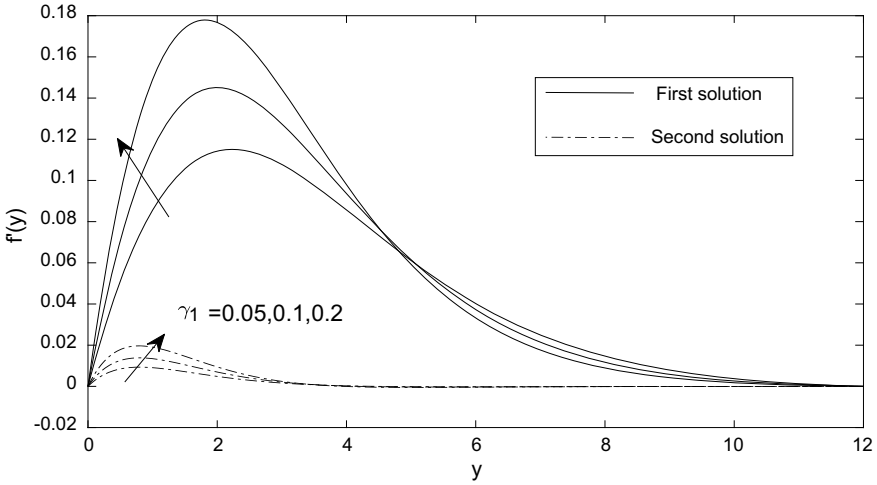

Fig. 4 Velocity distributions $f'(y)$ for some values of γ_1 when $\Pr = 0.7$ and $K = 2$

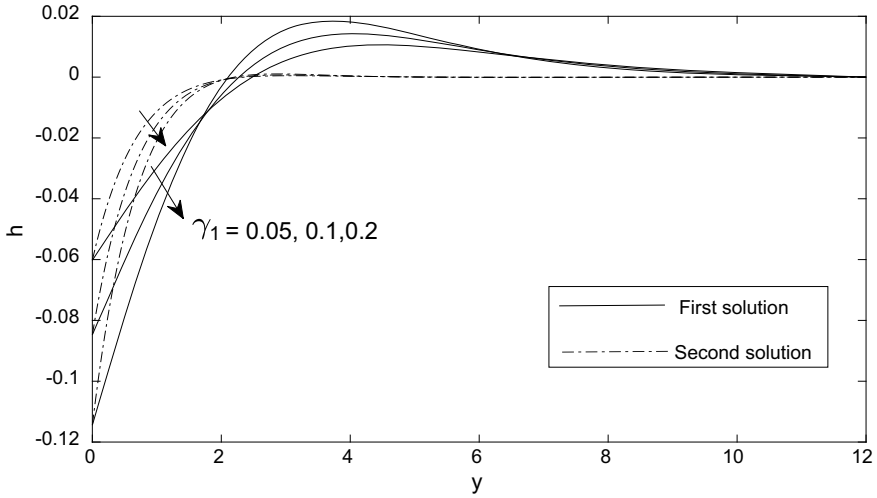

Fig. 5 Angular velocity distributions $h(y)$ for some values of γ_1 when $\Pr = 0.7$ and $K = 2$

Negative angular velocity of Newtonian fluid motion (first solution) indicates the reduction of angular displacement. Maximum variation of angular displacement is seen in the neighborhood of the surface where viscosity plays a significant role. Further, it may be concluded that magnitude of angular velocity reduces with the increase of K (Fig. 3). Physically, it may be interpreted that vortex viscosity reduces the angular momentum of governing fluid motion.

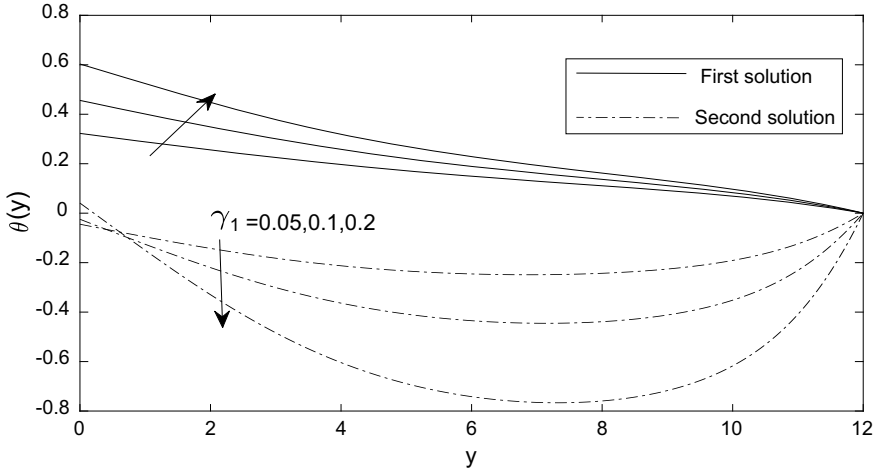

Fig. 6 Temperature distributions $\theta(y)$ for some values of γ_1 when $\Pr = 0.7$ and $K = 2$

Table 1 Numerical values of skin friction coefficient $f''(0)$

K↓	Alkasasbeh[a] et al. [18]		Present results			
			First solution		Second solution	
$\gamma_1 \rightarrow$	0.05	0.2	0.05	0.2	0.05	0.2
0	0.184661	0.357656	0.1846	0.3574	0.0150	0.0435
1	0.133231	0.244051	0.1427	0.2729	0.0283	0.0628
2	0.111617	0.195632	0.1205	0.2289	0.0312	0.0655

Table 2 Numerical values of wall temperature $\theta(0)$

K↓	Alkasasbeh[a] et al. [18]		Present results			
			First solution		Second solution	
$\gamma_1 \rightarrow$	0.05	0.2	0.05	0.2	0.05	0.2
0	0.149501	0.360667	0.1495	0.3606	0.4260	0.1258
1	0.157545	0.378091	0.1559	0.3726	0.4230	0.1233
2	0.162725	0.388925	0.1610	0.3820	0.0421	0.1218

Figures 4 and 5 represent the influences of the conjugate parameter γ_1 for $\Pr = 0.7$ and $K = 2$ on velocity and angular velocity distributions in the neighborhood of the lower stagnation point of the sphere. It is observed that fluid motion is accelerated with the conjugate parameter as the parameter (related with the heat transfer) helps to reduce the kinematic and vortex viscosities of fluid. Similarly, reduction in vortex viscosity also helps to reduce the magnitude of angular velocity of fluid.

Temperature distribution across the fluid flow is shown graphically in Fig. 6. During steady flow, there is continuous fall of temperature across the fluid flow, and the conjugate parameter enhances the temperature of fluid flow with maximum variation which is seen in the neighborhood of the surface. But, during time-dependent flow, the dimensionless temperature experiences negative values. Physically, it represents that free stream temperature is greater than temperature at the surface.

5 Conclusion

We have formulated the problem of micropolar fluid flow near the lower stagnation point with convection boundary condition. The MATLAB built-in bvp4c solver technique is used to solve the resulting problems. Some of the important results from the above investigations are highlighted below:

- When γ_1 and Pr are fixed, material parameter K helps to reduce the skin friction coefficient of steady flow (lower velocity gradient), but an opposite behavior is seen during unsteady fluid flow.
- The material parameter increases the wall temperature of steady flow, but it reduces the wall temperature during time-dependent flow.
- Fluid flow reaches its maximum speed in time-independent cases.
- Fluid flow attains its maximum variations with flow parameters in the boundary layer region.
- During unsteady flow, free stream temperature rises.
- For Newtonian fluid ($K = 0$), the steady and unsteady flow solutions of angular velocity experience completely negative values.

References

1. Eringen, A.C.: Theory of micropolar fluids. J. Math. Mech. **16**, 1–18 (1966)
2. Ariman, T., Turk, M., Sylvester, N.: Application of micro continuum fluid mechanics. Int. J. Eng. Sci. **12**, 273–293 (1974)
3. Rees, D.A.S., Bassom, A.P.: The Blasius boundary layer flow of a micropolar fluid. Int. J. Eng. Sci. **34**, 113–124 (1996)
4. Chen, T., Mucoglu, A.: Analysis of mixed force and free convection about a sphere. Int. J. Heat Mass Trans. **20**, 867–875 (1977)
5. Kasim, A.R.M., Mohammad, N.F., Aurangzaib, A., Shafie, S.: Natural convection boundary layer flow past a sphere with constant heat flux in viscoelastic fluid. J. Teknol. (2013)
6. Nazar, R., Amin, N., Grosan, T., Pop, I.: Natural convection boundary layer flow of a viscoelastic fluid on a solid sphere with Newtonian heating. Int. Commun. Heat Mass Trans **29**, 377–386 (2002)
7. Nazar, R., Amin, N., Grosan, T., Pop, I.: Free convection boundary layer on a sphere with constant surface heat flux in a micropolar fluid. Int. Commun. Heat Mass Trans. **29**, 1129–1138 (2002)

8. Cheng, C.Y.: Natural convection heat and mass transfer from a sphere in micropolarfluids with constant wall temperature and concentration. Int. Commun. Heat Mass Trans. **35**, 750–755 (2008)
9. Markin, J.: Natural-convection boundary-layer flow on a vertical surface with Newtonian heating. Int. J. Heat Fluid Flow **15**, 392–398 (1994)
10. Salleh, M.Z., Nazar, R., Pop, I.: Numerical solutions of free convection boundary layer flow on a solid sphere with Newtonian heating in a micropolar fluid. Meccanica **47**, 1261–1269 (2012)
11. Aziz, A.: A similarity solutions for laminar thermal boundary layer flow over a flat plate with a convective surface boundary condition. Commun. Nonlinear Sci. Numer. Simul. **14**, 1064–1068 (2009)
12. Makinde, O.D., Aziz, A.: MHD mixed convection from a vertical plate embedded in aporous medium with a convective boundary condition. Int. J. Therm. Sci. **49**, 1813–1820 (2010)
13. Ishak, A.: Similarity solutions for flow and heat transfer over a permeable surface with convective boundary condition. Appl. Math. Comput. **217**, 837–842 (2010)
14. Merkin, J.H., Pop, I.: The forced convection flow of a uniform stream over a flat surface with a convective surface boundary condition. Commun. Nonlinear Sci. Numer. Simul. **16**, 3602–3609 (2011)
15. Yao, S., Fang, T., Zhong, Y.: Heat transfer of a generalized stretching/shrinking wall problem with convective boundary conditions. Commun. Nonlinear Sci. Numer. Simulat. **16**, 752–760 (2011)
16. Yacob, N.A., Ishak, A.: Micropolar Fluid Flow over a Shrinking Sheet. Meccanica **47**, 293–299 (2012)
17. Mohamed, M.K.A., Salleh, M.Z., Nazar, R., Ishak, A.: Boundary Value Problems **1**, 1–10 (2013)
18. Alkasasbeh, H. T., Salleha, Mohd, Z., Tahar, R. M., Nazar, R., Pop, I.: Free convection boundary layer flow near the lower stagnation point of a solidsphere with convective boundary conditions in a micropolar fluid. AIP Conf. Proc. **1602**, 76–82 (2014)
19. SHU, J.J., Wilks, G.: Heat transfer in the flow of a cold, axisymmetric jet over a hot sphere. J. Heat Transfer-Trans. ASME **135**(3), 032201 (2013)
20. Aziz, L.A., Kasim, A. R. M., Salleh, M. Z. and Shafie, S.: Mixed convection boundary layerflow on a solid sphere in a viscoelastic micropolar fluid. In: Proceedings of the Third International Conference on Computing, Mathematics and Statistics (iCMS2017), (2019)
21. Ahmadi, G.: Self-similar solution of imcompressible micropolar boundary layer flow over a semi-infinite plate. Int. J. Eng. Sci. **14**, 639–646 (1976)
22. Weidman, P.D., Kubitschek, D.G., Davis, A.M.J.: The effects of transpiration on self-similar boundary layer flow over moving surfaces. Int. J. Eng. Sci. **44**, 730–737 (2006)
23. Khashi'ie, N.S., Arifin, N.Md., Rashidi, M.M, Hafidzuddin, E.H., Wahi, N.:Magnetohydrodynamics(MHD) stagnation point flow past a shrinking/stretching surface with double stratification effect in a porous medium. J. Thermal Ana. Calorimetry (2019)
24. Harris, S.D., Ingham, D.B., Pop, I.: Mixed convection boundary-layer flow near the stagnation point on a vertical surface in a porous medium: Brinkman model with slip. Transp. Porous Media. **77**, 267–285 (2009)